

Various Functionalities Based on Semiconductor Optical Amplifier for All-Optical Information Processing

Seok Lee*, Jae Hun Kim, Young Il Kim, Young Tae Byun,
Young Min Jhon, Deok Ha Woo, and Sun Ho Kim

*Photonics Research Center, Korea Institute of Science and Technology,
Seoul 130-650, KOREA*

(Received November 14, 2002)

By using a semiconductor optical amplifier and a cross-phase modulation wavelength converter, fundamental all-optical logic gates including NOT, AND, NOR, XOR, and XNOR have been newly proposed and implemented. Realization of these all-optical logic gates will bring up not only all-optical networks but also all-optical computing and signal processing.

OCIS codes : 200.0200, 190.0190.

I. INTRODUCTION

As the speed of telecommunication systems increases and reaches the limit of electronic devices, the demands for all-optical logic operations such as switching, decision-making, regenerating, and basic or complex computing are rapidly increasing. These fields have attracted extensive studies aimed at realizing all-optical logic gates that are the essential elements for optical signal processors. All-optical logic gates have the advantages of transparency and high-speed optical switching.

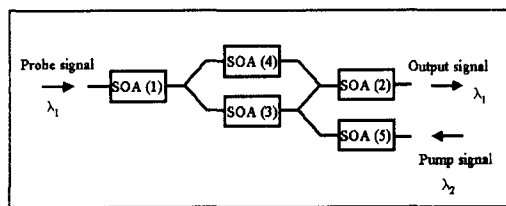
The optical logic gates may be classified into two types depending on the methodology used to achieve the nonlinear operation of the logic devices: the fiber nonlinearity-based logic gates and the semiconductor-optical-amplifier (SOA)-based logic gates. Many researchers have reported their own logic gates, which are NOR using a SOA [1], OR with NOR using an UNI (Ultrafast Nonlinear Interferometer) [2], XOR using a TOAD (Terahertz Optical Asymmetric Demultiplexer) [3], and so on. Even though logic gates using the UNI and the TOAD have the advantage of high-speed, they are very complex and difficult to integrate with other logic gates. Contrary to these devices, the SOA-based devices are compact, stable, integration capable, and potentially independent of polarization and wavelength [4]. Also, they have the advantages of a low switching energy and low latency [5]. In this paper, the SOA-based devices are basically employed to embody the fundamental logic functions including

logic NOT, AND, NOR, XOR, and XNOR.

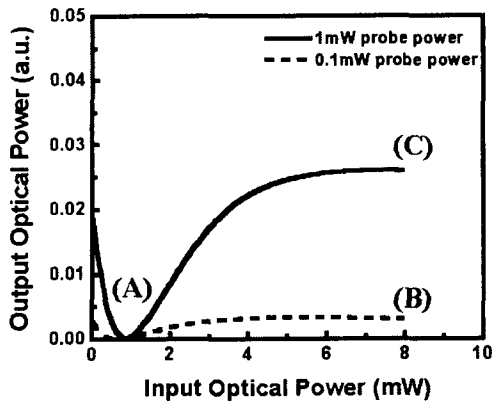
II. ALL-OPTICAL SWITCHING BY USING XGM AND XPM

To realize the all-optical logic gates, cross-phase modulation (XPM) and cross-gain modulation (XGM) are mainly employed. Both effects can be obtained by using the SOA-based devices. However, working mechanisms are quite different. Here are brief descriptions of XPM and XGM.

XPM can be explained with static characteristics of the XPM wavelength converter in Fig. 1. The XPM wavelength converter utilized in this paper consists of 5 SOAs. Mainly two SOAs that are SOA (3) and SOA (4) are used for signal interference to cause cross-phase modulation. Three extra SOAs are used only for amplifying the input and output signals; they do not affect basic operation of cross-phase modulation. When proper currents are applied to each of the SOA's, pump signal injected into an arm of the XPM wavelength converter can change the carrier density of the SOA (3) in the interferometer structure, producing a change of refractive index in the SOA (3). This in turn leads to the phase change of an injected probe beam. Since SOA (4) is only affected by the probe signal while SOA (3) is affected by both signals, a phase difference between SOA (4) and SOA (3) occurs. Signals from SOA (4) and SOA (3) are coupled together to form the output signal. The intensity of output signal is altered owing to the interference of two beams



(a)

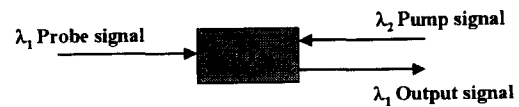


(b)

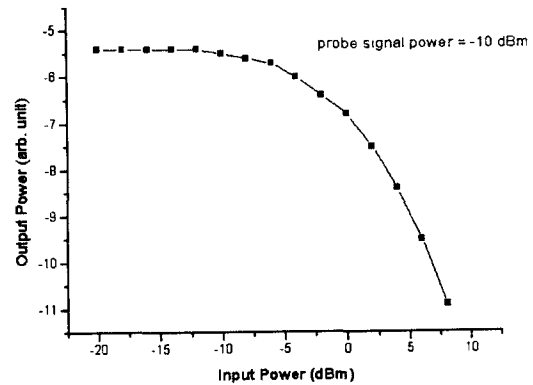
FIG. 1. Wavelength conversion by XPM in the XPM wavelength converter. (a) Scheme to realize wavelength conversion by XPM. (b) Static characteristics of XPM.

with different phase as the injected pump power is increased [6]. When the power of the pump signal varies, the output signal moves along the static transfer characteristics. Output of the XPM wavelength converter also depends on the intensity of the probe signal. To verify the effects of different probe signal intensities, the probe signal intensities of 1 and 0.1 mW have been applied. When a probe signal with 1 mW is injected into the XPM wavelength converter, power level of the static transfer characteristics is much higher than that with probe signal intensity of 0.1 mW. The effects of probe signal intensity are clearly shown in Fig. 1(b).

XGM can be explained with static characteristics of the SOA in Fig. 2. The Pump signal can be composed of logic 1 state with relatively high power and logic 0 state with low power. When the pump signal is passed into the SOA, carrier depletion in the SOA occurs for the case of logic 1. This causes the gain saturation of the SOA [7]. When probe signal with continuous wave (CW) light is coupled into the SOA, it encounters carrier depletion caused by the pump signal. Therefore, the probe signal in the SOA will experience the lower gain in logic 1 state of pump signal than in logic 0 state: the output signal turns into the reversed signal of the pump signal. Thus, amplitude inversion of the signal is obtained [8].



(a)



(b)

FIG. 2. Wavelength conversion by XGM in the SOA. (a) Scheme to realize wavelength conversion by XGM. (b) Static characteristics of XGM.

III. ALL-OPTICAL LOGIC GATES BASED ON XPM

1. All-Optical AND Gate

To accomplish an all-optical AND logic gate, the cross-phase modulation (XPM) wavelength converter (Alcatel 1901 ICM) has been utilized [9]. The XPM wavelength converter is utilized to perform logic AND for the first time by using the definable binary points of probe and pump signals. The operation of the all-optical AND gate can be fully explained with Fig. 1(b). When high power of the probe signal is coupled into the XPM wavelength converter, the power of the output signal increases as the power of the pump signal intensifies. Also, when low power of the probe signal passes through the XPM wavelength converter, the power of the output signal is small enough to be considered as signal zero regardless of pump signal intensity variation. The position of the output signal is located in (C) when both pump and probe signals have high power. If probe signal has low power, the position of the output signal is located in either (A) for pump signal with low power or (B) for pump signal with high power. For either case, the output signal has low power. Therefore, the AND characteristic is verified since the output has high power only for both input signals with high power.

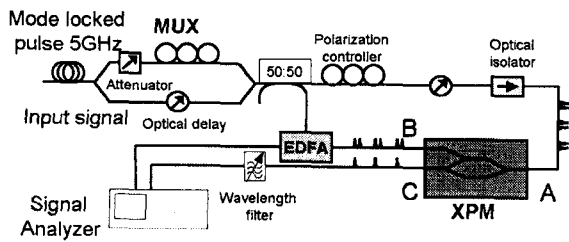


FIG. 3. Experimental set-up for the all-optical AND gate at 20 Gb/s by using the XPM wavelength converter.

The experimental setup is shown in Fig. 3. A mode locked fiber ring laser with the frequency of 5 GHz has been used to generate the RZ pattern signal. Signal with the wavelength of 1549 nm and pulse width of less than 15 ps is divided by a 50:50 coupler and recombined by the other 50:50 coupler after applying 50 ps delay for one arm to form signal A with the pattern of 1100. Delay of one bit is applied to signal A to generate signal B with pattern of 0110. Signal B is amplified up to proper power level by an EDFA (Erbium doped fiber amplifier).

Signals A and B are coupled into the XPM wavelength converter to procure the AND gate signal. The input and output signals are configured in Fig. 4. Overlapping signal A adjusted by delay line with 0110 of signal B produces output signal with the pattern of 0100, which is the correct proof for characteristics of AND logic gate. Therefore, the all-optical AND gate has been successfully demonstrated at 20 Gb/s.

To investigate the effect of recovery time of the SOA in the XPM wavelength converter, signal B is delayed up to 100 ps, which is covered for the duration of 2 bits, compared to signal A. The output signal performing evident logic AND is maintained for about 15 ps. The temporal window within which the output signal maintains higher than its half value is about 50ps. This may be the sum of duration time of the pump signal pulse and recovery time of the SOA.

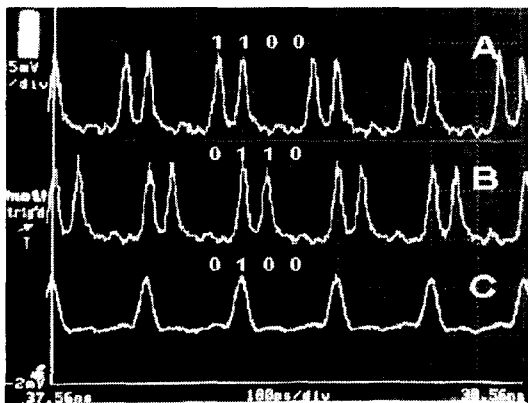
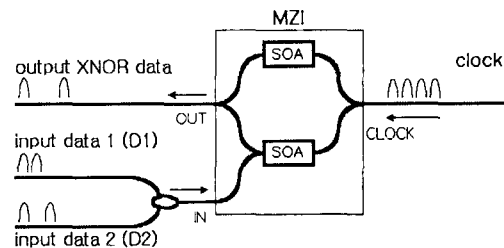


FIG. 4. Demonstration of 20 Gb/s all-optical AND gate by using the XPM wavelength converter.

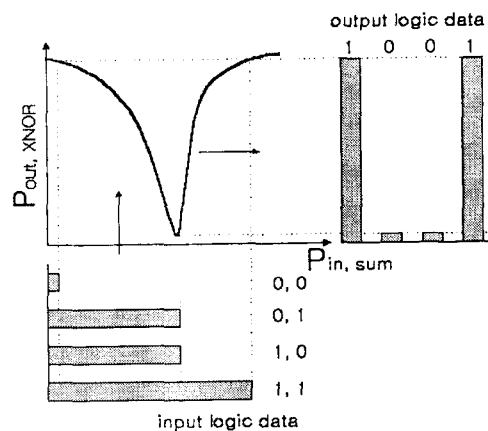
2. All-Optical XNOR Gate

By using the XPM wavelength converter, an all-optical XNOR gate has been demonstrated at 10 Gb/s [10]. Fig. 5 shows a schematic diagram of the proposed XNOR gate detailing the principle of operation, and the characteristic function of the XNOR gate describing the relationship between the input and output signals.

The whole operation can be depicted by the characteristic curves in Fig. 5(b). The power level of the output signal corresponds to the logical XNOR: (1) the logical 'ONE' when both input signals are either pulses or spaces simultaneously, and (2) the logical 'ZERO' when two input signals have a different power level from each other, a space and a pulse. It is noted that the residual output pattern for 'ZERO' in the output logic data can be removed by using a threshold device [11]. Fig. 6 shows a schematic diagram of the experimental system for the proposed all-optical XNOR gate based on the XPM wavelength converter. The mode-locked pulse laser is used as an optical pulse



(a)



(b)

FIG. 5. Principle of all-optical XNOR logic gate by using the XPM wavelength converter. (a) Schematic diagram of the XPM wavelength converter as XNOR logic gate. (b) Illustration of the principle of operation: the characteristic function of the XNOR gate.

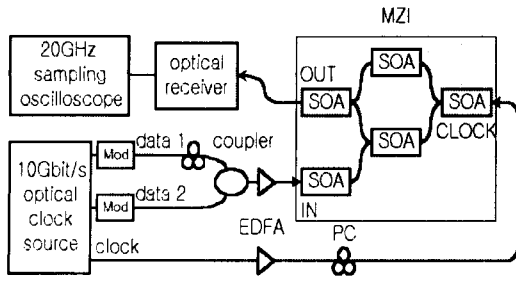


FIG. 6. Experimental setup for 10 Gb/s XNOR logic gate by using the XPM wavelength converter PC: polarization controller Mod: LiNbO₃ modulator.

source, which generates 10 Gb/s return to zero (RZ) pulses with a pulse width of about 20 ps at the wavelength of 1549 nm. The pulse stream is modulated by using LiNbO₃ modulators to generate two arbitrary data patterns.

Fig. 7 shows the experimental results of the proposed all-optical XNOR gate. Fig. 7(a)-7(d) represent the 10 GHz input clock pulses, the input data D1 with the data pattern of 1100, the input data D2 with the data pattern of 1010, and the resulting output of logic XNOR data with the data pattern of 1001, respectively. The results in Fig. 7 clearly show that the proposed all-optical XNOR gate is operable, and appropriately generates the output pattern according to logic XNOR. The residual small peaks in the output stream can be suppressed by using a threshold device.

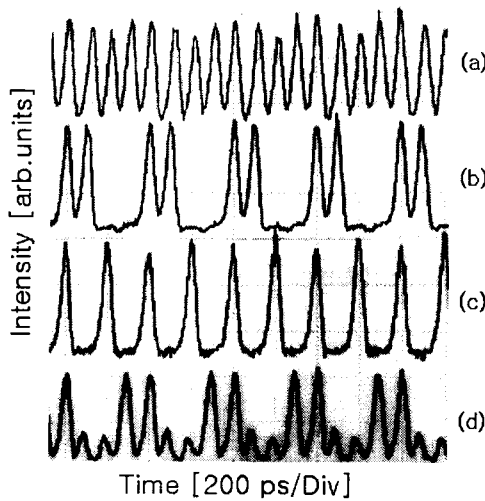


FIG. 7. Experimental results of all-optical XNOR logic gate by using the XPM wavelength converter. (a) Input clock pulses at 10 GHz. (b) Input data 1 with data pattern of 11001100 (c) Input data 2 with data pattern of 10101010 (d) Output XNOR logic data with data pattern of 10011001

IV. ALL-OPTICAL LOGIC GATES BASED ON XGM

1. All-Optical NOT Gate

By using gain saturation and nonlinearity of the SOA, gain inversion can be performed [12]. Gain saturation effect of the SOA, which is called XGM, is employed. Even though XGM is already demonstrated in [7], an all-optical NOT gate in this paper is quite different from previous results. In this paper, speed limitation reported by previous NOR gates is overcome by using the clock signal for a probe signal instead of a continuous wave (CW) light. The main mechanism in this paper is that the clock signal as probe signal does not need to be returned back to the logic 1 state in the SOA. The SOA is used for gain saturation-purpose only by the pump signal while the SOAs in previous NOR gates are being used as both saturation-purpose and gain recovery medium. This removes the slow gain recovery time of about 300 ps. Also, the probe signal with CW light is substituted by a clock signal for high-speed operation. The high-speed all-optical NOT gate using a clock pulse signal is demonstrated for the first time.

Configuration of the experimental set up for an all-optical NOT gate is shown in Fig. 8 [8]. The mode locked fiber ring laser with the frequency of 10 GHz has been utilized to generate the signal with the wavelength of 1549 nm. The signal from the mode locked fiber ring laser is divided by the 50:50 coupler and recombined by the other 50:50 coupler after applying a delay of 50 ps for one arm to generate a clock signal. Clock signal and signal A have been injected into the SOA for carrier depletion and output amplitude inversion, which is logic NOT. Input A, clock and output signals are displayed in Fig. 9. As expected, output pulses are only observed while pulses of signal A do not exist. Therefore, the all-optical NOT gate using the SOA is successfully demonstrated at 20 Gb/s.

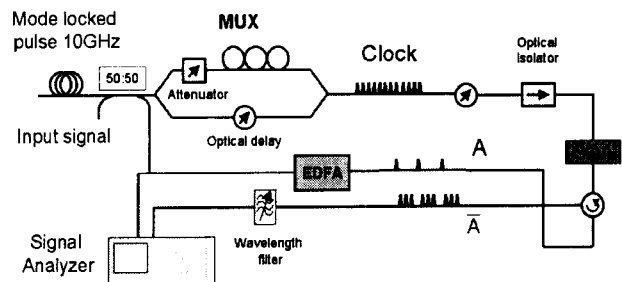


FIG. 8. Experimental set-up for the all-optical NOT gate by using the SOA.

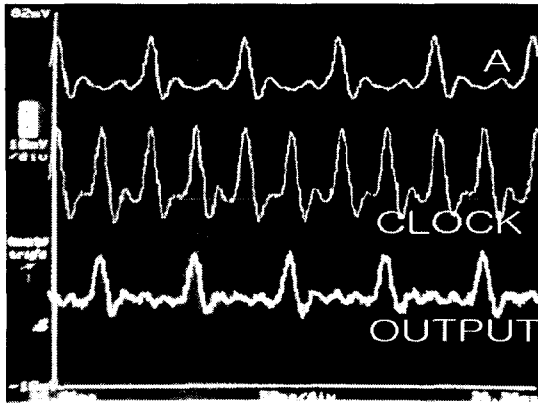


FIG. 9. Demonstration of 20 Gb/s all-optical NOT gate by using the SOA.

2. All-Optical NOR Gate

By using the gain saturation effect used for the all-optical NOT gate, an all-optical NOR gate has been demonstrated [13]. Configuration of the experimental set up is shown in Fig. 10. External modulation for signal generation is utilized while the direct modulation of signals is being used in [1]. For the external modulation, the input signals are only used at the first gates of cascaded logic systems. With the internal modulation, signals for each individual gate are required. Also, power and timing synchronization among the generated signals for each gate is also required. Therefore, the external modulation method for signal generation is utilized for integration possibility with other gates. By using a pulse generator and a Mach-Zehnder Modulator, the signal from a distributed feedback (DFB) laser diode (LD) has been modulated with the external modulation method to form signal A with the pattern of 1100. Signal A has been divided into two parts, and delay of one bit has been applied to form signal B with the pattern of 0110.

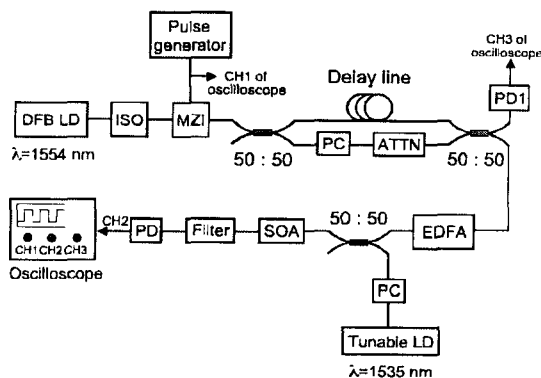


FIG. 10. Experimental set-up for the all-optical NOR gate by using the SOA.

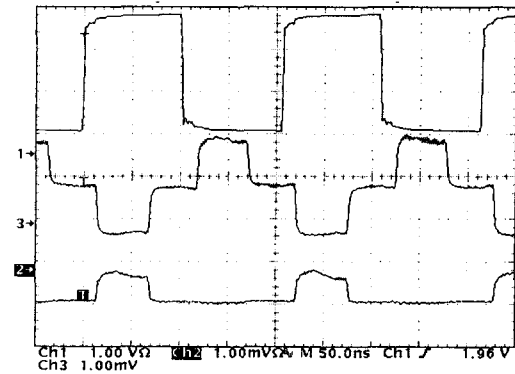


FIG. 11. Demonstration of the all-optical NOR gate by using the SOA.

Then, two parts of the pulse signal are added to form the signal set of (0,0), (1,0), (1,1), and (0,1). The Probe signal of CW light from a tunable LD and signal A+B are injected into the SOA. Due to the gain saturation effect of the SOA, the output signal has a logic state of 1 when only (0,0) of input appears. Input and output signals are seen in Fig. 11. As shown in Fig. 11, output only has logic 1 when both inputs A and B are logic 0. Otherwise, output has logic 0. Since these results coincide with logic NOR, the all-optical NOR gate has been successfully demonstrated.

However, the operational speed of the all-optical NOR gate using the signals with NRZ pattern and CW light is limited to several hundred Mb/s. When logic 1 state is continued for the output signal with NRZ pattern, the signal does not return to logic 0 state. Also, the output signal should recover the gain when the output signal changes from logic 0 to logic 1. In this process, recovery time of more than 200 ps in the SOA is expected. If the distance between pulses is less than 200 ps, overlapping between output signal pulses occurs. This results in serious output signal degradation. This problem can be solved by two methods.

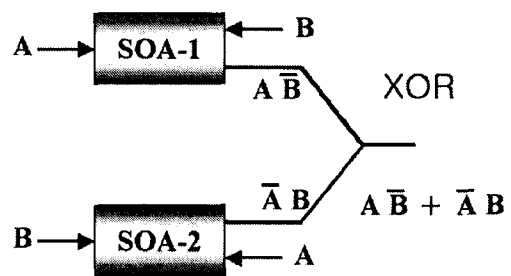


FIG. 12. The scheme of the all-optical XOR gate by using two SOAs.

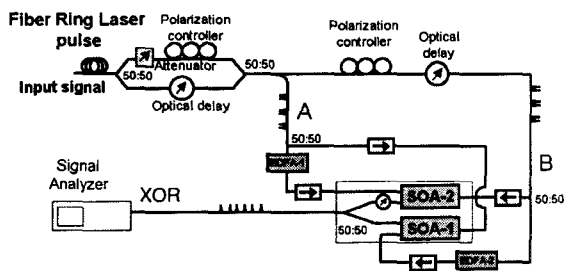


FIG. 13. Experimental setup for the all-optical XOR gate by using two SOAs.

The first method is to use the SOA with high photon density in the active region [14]. The other method is to decrease the recovery time dependency by using the signals with RZ pattern and the clock signal with continuous logic 1 state.

3. All-Optical XOR Gate

By using two SOAs, an all-optical XOR gate has been demonstrated at 10 Gb/s [15]. Gain saturation effect of SOA, which is called XGM, is employed. By passing signal A as probe signal and signal B as pump signal into the SOA, Boolean $A\bar{B}$ can be obtained. Also, by changing the role of signals A and B, Boolean $\bar{A}B$ can be acquired. As shown in Fig. 12, addition of Booleans $A\bar{B}$ and $\bar{A}B$ results in Boolean $A\bar{B} + \bar{A}B$, which is logic XOR.

Fig. 13. shows the experimental setup for realizing the all-optical XOR gate. The mode-locked fiber ring laser incorporated with the pulse generator has been used to generate the pulse with 400 ps repetition rate. 2.5 Gb/s signal is divided by a 50:50 coupler

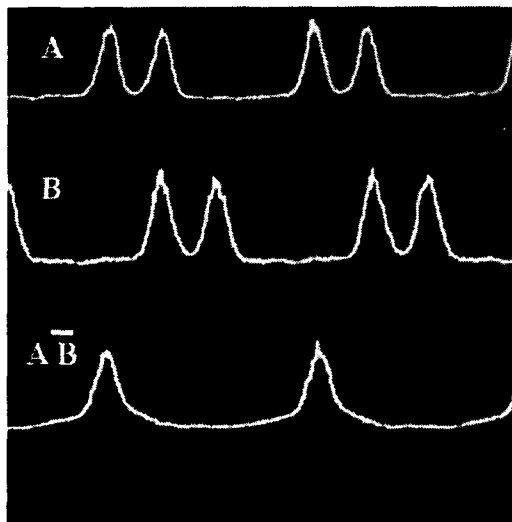


FIG. 14. Realization of Boolean $A\bar{B}$ by using SOA-1.

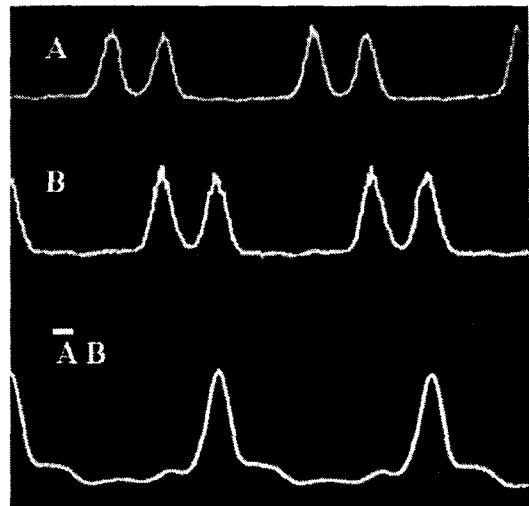


FIG. 15. Realization of Boolean $\bar{A}B$ by using SOA-2.

and recombined by another 50:50 coupler after applying the delay for one arm to form signal A with the pattern of 1100. The delay of one bit is applied to signal A to generate signal B with the pattern of 0110. By passing signal A as probe signal and signal B as pump signal into SOA-1, Boolean $A\bar{B}$ (Fig. 14) has been obtained. Also, by switching the roles of signal A and B for SOA-2, Boolean $\bar{A}B$ (Fig. 15) has been acquired. After combining Boolean $A\bar{B}$ and $\bar{A}B$ with the 50:50 coupler, the output signal has been detected and displayed on the signal analyzer. Fig. 16 depicts the added signal of Boolean $A\bar{B}$ and $\bar{A}B$ which is Boolean $A\bar{B} + \bar{A}B$. As shown in Fig. 16, the output signal is logic 1 when either signal A or B is logic 1. When both signals A and B are logic 0 or 1, the

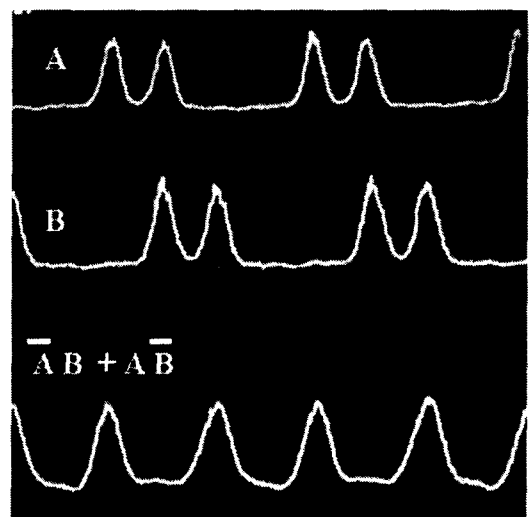


FIG. 16. The all-optical XOR gate; Boolean $A\bar{B} + \bar{A}B$, the addition of Boolean $A\bar{B}$ and $\bar{A}B$.

output signal is logic 0. These results coincide with logic XOR. Therefore, the all-optical XOR gate at 10 Gb/s has been successfully realized.

The extinction ratio of the XOR gate was measured to be 11 dB. The polarization dependence of the XOR gate has been investigated by observing the output signal while changing the polarization states of the input signals A and B by adjusting the two polarization controllers. The output signal remained invariant within 5%, hence implying that the XOR gate operation is polarization independent.

V. CONCLUSION

In this paper, all-optical logic gates including AND, XNOR, NOT, NOR, XOR by using the SOA-based devices are demonstrated. XPM of the XPM wavelength converter is used for the all-optical AND and XNOR gates while XGM of the SOA is utilized for the all-optical NOT, NOR, and XOR gates. It is advantageous to use the SOA-based devices in that they are compact, stable, integration capable, and potentially independent of polarization and wavelength. Also, they have the advantages of a low switching energy and low latency. Realization of the all-optical logic gates will bring up not only the increased speed and capacity of telecommunication systems, but also the various functionalities including packet switching, decision making, regenerating, and basic or complex computing.

*Corresponding author : slee@kist.re.kr.

REFERENCES

- [1] A. Sharaiha, H. W. Li, F. Marchese, and J. Le Bihan, *Electron. Lett.* **33**, 323 (1997).
- [2] N.S. Patel, K. L. Hall, and K. A. Rauschenbach, *Opt. Lett.* **21**, 1466 (1996).
- [3] A. J. Poustie, K. J. Blow, Kelly, and R. J. Manning, *Opt. Commun.* **156**, 22 (1998).
- [4] T. Fjelde, D. Wolfson, A. Kloch, B. Dagens, A. Coquelin, I. Guillemot, F. Gaborit, F. Poingt, and M. Renaud, *Electron. Lett.* **36**, 1863 (2000).
- [5] K. Vlachos, K. Zoiros, T. Houbavlis, A. Hatziefremidis, and H. Avramopoulos, *Proc. LEOS 768*, 2 (1999).
- [6] C. Joergensen, S. L. Danielsen, T. Durhuus, B. Mikkelsen, K. E. Stubkjaer, N. Vodjdani, F. Ratovelomanana, A. Enard, G. Glastre, D. Rondi, and R. Blondeau, *IEEE Photon. Technol. Lett.* **8**, 521 (1996).
- [7] T. Durhuus, B. Mikkelsen, C. Joergensen, S. L. Danielsen, and K. E. Stubkjaer, *J. Lightwave Technol.* **14**, 942 (1996).
- [8] J. H. Kim, B.-K. Kang, Y. H. Park, Y. T. Byun, S. Lee, D. H. Woo, S. H. Kim, and S. S. Choi, in *Contemporary Photonics Technology '01 (Communications Research Laboratory, Tokyo, Japan, 2001)*
- [9] B. K. Kang, J. H. Kim, Y. T. Byun, S. Lee, Y. M. Jhon, D. H. Woo, J. S. Yang, S. H. Kim, Y. H. Park, and B. G. Yu, *Jap. J. Appl. Phys.* **41**, L568 (2002).
- [10] S. C. Lee, J. W. Park, K. C. Lee, D. S. Eom, S. Lee, and J. H. Kim, *Jap. J. Appl. Phys.* **41**, L1155 (2002).
- [11] A. J. Poustie, K. J. Blow, and R. J. Manning, *Opt. Commun.* **146**, 262 (1998).
- [12] A. Kloch, P. B. Hansen, D. Wolfson, T. Fjelde, and K. Stubkjaer, *IEICE Trans. Electron.* **E82-C**, 1475 (1999).
- [13] Y. T. Byun, S. H. Kim, D. H. Kim, D. H. Woo and S. H. Kim, *Sae Mulli*, **40**, 560 (2000).
- [14] S. L. Danielsen, C. Joergensen, M. Vaa, K. E. Stubkjaer, P. Doussiere, F. Pommereau, L. Goldstein, R. Ngo, and M. Goix, in *Optical Fiber Communication '96 (Optical Society of America, San Jose, USA) PD12*.
- [15] J. H. Kim, Y. M. Jhon, Y. T. Byun, S. Lee, D. H. Woo, and S. H. Kim, *IEEE Photon. Technol. Lett.* **14**, 1436 (2002).